Experimental and parametric evaluation of cut quality characteristics in CO 2 laser cutting of polystyrene

Haddadi, E., Moradi, M., Karimzad Ghavidel, A., Karimzad Ghavidel, A. & Meiabadi, S.

Original citation & hyperlink:
Haddadi, E, Moradi, M, Karimzad Ghavidel, A, Karimzad Ghavidel, A & Meiabadi, S 2019, 'Experimental and parametric evaluation of cut quality characteristics in CO 2 laser cutting of polystyrene', Optik, vol. 184, pp. 103-114.
https://dx.doi.org/10.1016/j.ijleo.2019.03.040

DOI 10.1016/j.ijleo.2019.03.040
ISSN 0030-4026

Publisher: Elsevier

Experimental and Parametric Evaluation of Cut Quality Characteristics in CO_2 Laser Cutting of Polystyrene

Elyas Haddadi[1], **Mahmoud Moradi**[2, 3*], **Ayub Karimzad Ghavidel** [1], **Ali Karimzad Ghavidel** [1], **Saleh Meiabadi**[4]

1- Department of Engineering Science, Faculty of Tabriz, Tabriz Branch, Technical and Vocational University (TVU), Tabriz, Iran
2- Department of Mechanical Engineering, Faculty of Engineering, Malayer University, Malayer, Iran
3- Laser Materials Processing Research Center, Malayer University, Malayer, Iran
4- Department of Mechanical Engineering, École de Technologie Supérieure, Canada 1100 Notre-Dame West, Montreal, QC, H3C 1K3, Canada

Abstract
Cutting characteristics such as heat affected zone (HAZ), top and bottom kerf widths, ratio of top kerf width to bottom kerf width, and dross height are so reliant on process condition in the laser cutting of polymer materials. In the present research, a 60 (W) continuous wave CO_2 laser cutting machine was used for cutting the extruded samples of Polystyrene sheet with the thickness of 3 mm. The experiments were designed based on the statistical method, design of experiments. Three variables considered as process parameters including laser power (in three level of 60, 70 and 80 Watts), cutting velocity (in three level of 6, 10, 14 mm/s) and cutting with covering gas or without gas. The results indicated that the maximum feasible laser power and increasing cutting velocity using compressed air resulted in decreasing HAZ width. By gradual increase of the laser power the cutting mechanism converts from melting to evaporation. Increasing laser power and cutting velocity individually made the dross height smaller. The process parameters were optimized to achieve minimum top kerf width, minimum HAZ width, and ratio equal to 1.

Keywords
Laser Cutting; Polystyrene; Heat Affected Zone; Dross Height; Design of Experiments.

1. Introduction
Laser cutting is one of the most widely used modern machining methods thanks to several advantages namely high production speed, system flexibility, no need to specific fixtures, no tool wear, no vibration, and no need to clamping parts [1-7]. Laser cutting is a non-contact process which has low cost, high precision and is used for many applications, while laser cutting quality is greatly affected by the process parameters [8-14]. CO_2 laser cutting is also one of the common methods of producing polymeric sheets. Several studies have been conducted to control cutting process more accurately and precisely in order to produce high quality parts. Different outputs such as heat affected zone (HAZ), dross height, surface roughness, the top and bottom kerf widths, laser penetration depth, cutting edges angle, and mechanical properties of cutting parts are among the parameters which have been investigated by the researchers [9, 15]. Nonetheless, the mechanical properties of the produced parts, such as tensile strength and stiffness, could also be considered as output [16]. One of the earlier studies in this field was done in 2004, the most important finding was the possibility of cutting non-metallic materials with low-power laser (60 Watts) [17]. In numerous researches, the common point is the high dependence of outputs on material properties and the cutting process parameters [4]. It has been proved that laser power and cutting velocity play the major roles in the cutting qualities [18]. However, thermal properties of the materials and the mechanism of cutting have a great influence on cutting characteristics. There are two different cutting mechanisms depending on cutting circumstances. The first mechanism is the melting of the material at the cutting area under the laser beam and its discharge from the base material by covering gas. The second mechanism is the direct sublimation of the material at the cutting area with laser beam radiation and its turning into a gas phase. Moreover, sometimes combination of these mechanisms is observed. Cutting of materials by

melting mechanism is very challenging and problematic because melted material removes from the base material by the covering gas, while some parts of removed melt cling to the cutting edges and all the outputs are affected by its undesirable effects [19]. In a recent study by Karimzad Ghavidel et al. [20] it has been demonstrated that in the laser cutting process with the dominant mechanism of melting, changing the process parameters, including the laser power and cutting velocity, leads to control outputs of the process efficiently. Polystyrene is an engineering polymer with many advantages and worthwhile in various industries [21-24]. The production of two-dimensional polystyrene sheets using the laser cutting process is one of the industry's challenges due to its thermal properties.

To improve the cutting condition of polystyrene, investigating the laser power and cutting velocity, as well as covering gas pressure is the path ahead. According to literature, there has not been a comprehensive study on the laser cutting of the polystyrene sheet. Due to the wide range of applications of this polymer and the vast capabilities the laser materials processing, it seems essential to carefully study the laser cutting of polystyrene, in order to produce high quality and more precise parts. Therefore, the purpose of this study is to determine the optimal process parameters of the laser cutting process of the polystyrene sheet by investigating laser power, cutting velocity and covering gas based on the full factorial experiments. To achieve this goal, the effects of laser power, cutting velocity and covering gas on the width of HAZ, top and bottom kerf widths, ratio, and dross height were evaluated by response surface method.

2. Experimental Work and Methodology

Polystyrene sheets with dimensions of 3 × 200 × 400 mm were the material of this research and are produced by using an Aida plastic–co extrusion machine. The mechanical and physical properties of polystyrene are presented in Table 1.

Table 1. Mechanical and physical characteristics of polystyrene

Property	Unit	Amounts
Elastic Module	GPa	3
Tensile strength	MPa	30
Maximum elongation	%	3
Bending strength	MPa	76
Bending Module	GPa	3.2
Density	g/cm^3	1.05
Melt flow index (MFI)	g/10 min	11
Thermal conductivity	W/mk	0.14
Transparency	%	98
Absorbance at 1024nm	Au	0.01

Laser cutting of samples is accomplished by a 120W continuous CO_2 laser system (YM Laser Machine PN1380) and a two axes CNC controlled table. It was also proved that the best surface quality could be obtained when the focal point is located in middle of the part thickness (FPP= -1.5 mm). The nozzle diameter was 20 mm and the focused beam diameter was 0.2 mm. Geometrical features of the cross-section of the kerf is depicted in Figure 1-a. The cutting line was selected as a 6 mm straight line as shown in Figure 1-b. Progressive movements were made by the laser nozzle and the plastic sheet was fixed. In order to determine levels of laser power and cutting velocity, primary tests were performed and the levels were selected provided that the complete cut happened. The heat affected zone and the top and bottom kerf widths were measured by light microscopy of metallurgy manufactured by the SAIRAN Company with a magnification of 100 times and 0.01 mm accuracy. The dross height (at five points) was measured by a micrometer of 0.01 mm resolution made by Mitutoyo.

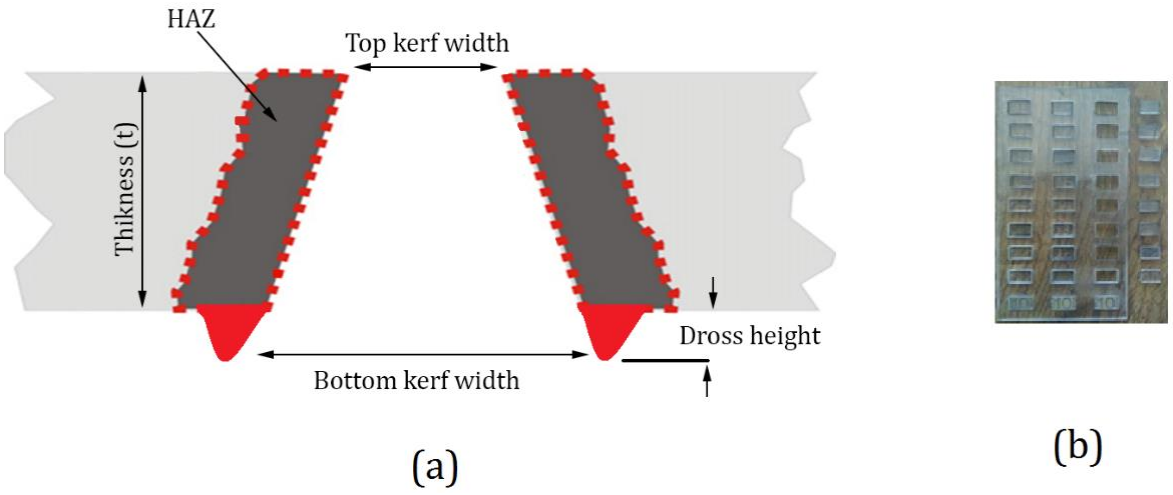

Fig. 1. a) Geometrical features of the cross-section of the kerf b) The laser cutting samples (cutting line is 6 mm)

In this research, laser power (W), cutting velocity (mm/s) and cutting with covering gas or without gas were considered as independent input parameters. The covering gas was a compressed air with a blast pressure of 1.5 bar. Table 2 shows three input variables of the experiment, coded values and actual values of their levels. Experimental layout and results are presented in Table 3 which shows that the design includes 18 experiments. The width of HAZ, top and bottom kerf widths, ratio, and dross height are selected as response variables. For each experiment, the results were repeated seven times, and the average of the seven results was reported as the final result of the experiments.

Table 2. Independent variables with design levels

Variable	Notation	Unit	-1	0	1
Gas Condition	G	[---]	Without gas	------	With gas
Laser power	P	[W]	60	70	80
Cutting velocity	V	[mm/s]	6	10	14

Table 3. Experimental layout and results

No	Input Parameters			Output Results				
	Gas Condition	Laser Power (W)	Cutting Velocity (mm/s)	width of HAZ (mm)	Top kerf width (mm)	Bottom kerf width (mm)	Ratio	Dross height (mm)
1	With gas	80	14	0.027	0.350	0.418	0.8373	0.033
2	With gas	80	10	0.036	0.340	0.480	0.7083	0.040
3	With gas	80	6	0.037	0.430	0.603	0.7127	0.060
4	With gas	70	14	0.035	0.310	0.410	0.7561	0.056
5	With gas	70	10	0.036	0.340	0.450	0.7555	0.066
6	With gas	70	6	0.037	0.400	0.590	0.6779	0.100
7	With gas	60	14	0.038	0.333	0.393	0.8474	0.070
8	With gas	60	10	0.046	0.340	0.450	0.7555	0.110
9	With gas	60	6	0.057	0.430	0.580	0.7414	0.240
10	Without gas	80	14	0.064	0.460	0.580	0.7931	0.050
11	Without gas	80	10	0.075	0.513	0.673	0.7624	0.090

12	Without gas	80	6	0.085	0.540	0.770	0.7013	0.170
13	Without gas	70	14	0.087	0.450	0.490	0.9183	0.070
14	Without gas	70	10	0.089	0.470	0.520	0.9038	0.106
15	Without gas	70	6	0.103	0.500	0.690	0.7246	0.160
16	Without gas	60	14	0.094	0.340	0.450	0.7555	0.0 63
17	Without gas	60	10	0.101	0.440	0.480	0.9166	0.130
18	Without gas	60	6	0.108	0.450	0.500	0.9	0.270

3. Results and discussion

3.1. Heat affected zone (HAZ) width

The HAZ is visible by a microscope because its color is darker than the base material. Images of the HAZ in different cutting conditions for a number of samples are shown in Fig. 2. The HAZ formation depends on the thermal properties of materials such as the thermal conductivity and thermal penetration coefficients. Both melting and vaporization mechanisms are expected in the polymer laser cutting. The analysis of variance for HAZ width, Table 4, reveals that covering gas is the most important controlled variables for HAZ width.

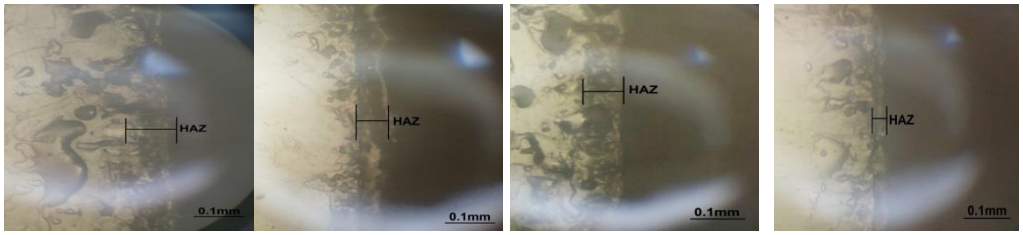

P=60W, V=6mm/s, G=yes *P*=60W, V=6mm/s, G=No *P*=60W, V=14mm/s, G=yes P=60W, V=14mm/s, G=No

Fig. 2. The microscopic images of HAZ

Table 4. Analysis of variance (ANOVA) for HAZ width

Source	Sum of Squares	Df	Mean Square	F Value	p-value
Model	0.062	3	0.021	244.01	<0.0001
G	0.054	1	0.054	639.11	<0.0001
P	5.267E-003	1	5.267E-003	62.58	<0.0001
V	2.552E-003	1	2.552E-003	30.32	<0.0001
Residual	1.178E-003	14	8.417E-005		
Total	0.063	17			
	R-Squared= 98.12%			R-Squared (Adj)= 97.72%	

Equations (3) and (4) are predictive model of HAZ width in terms of coded and actual factors, respectively:

$$(\text{HAZ Width})^{0.34} = +0.38 - 0.055\ G - 0.021\ P - 0.015\ V \quad (3)$$

$$(\text{HAZ Width})^{0.34} = +0.56758 - 0.054667\ G - 2.09511E\text{-}003\ P - 3.64601E\text{-}003\ V \quad (4)$$

The coded equation indicates that covering gas coefficient is greater than other coefficients. Figure 3 demonstrates perturbation plot of HAZ width which helps to compare effects of all the factors in the central point in the design space. The figure illustrates that increasing each of input factors while holding the other factors constant results in decreasing HAZ width. Figure 4 shows 3D surface plots of HAZ width in terms of input parameters. To explain the 3D surface plots it can be noted that by increasing laser power, the cutting mechanism turns from melting mode to direct evaporation mode. In this case, the cutting line is rapidly discharged and the interaction between the laser beam and the cutting walls decreases, and as a result, the time required to make structural changes in the cutting

edges is limited and, eventually, the width of the area decreases. Likewise it is observed that with increasing the cutting velocity, the heat affected zone width decreased. Comparing two modes of using or not using covering gas, it is observed that the HAZ is significantly reduced by covering gas. These findings show that the use of covering gas transforms the mechanism of cutting from melting to evaporation. In addition, the covering gas causes faster discharge of the melted material from the cutting line and reduces the heat transfer time to the walls.

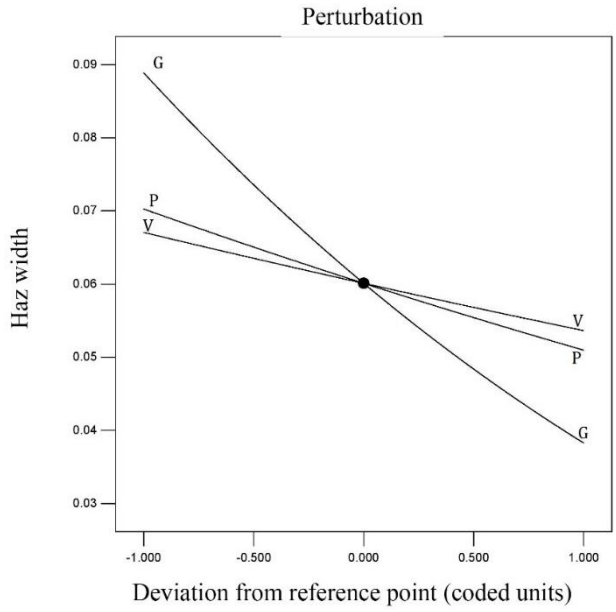

Fig. 3. Perturbation plot of HAZ width

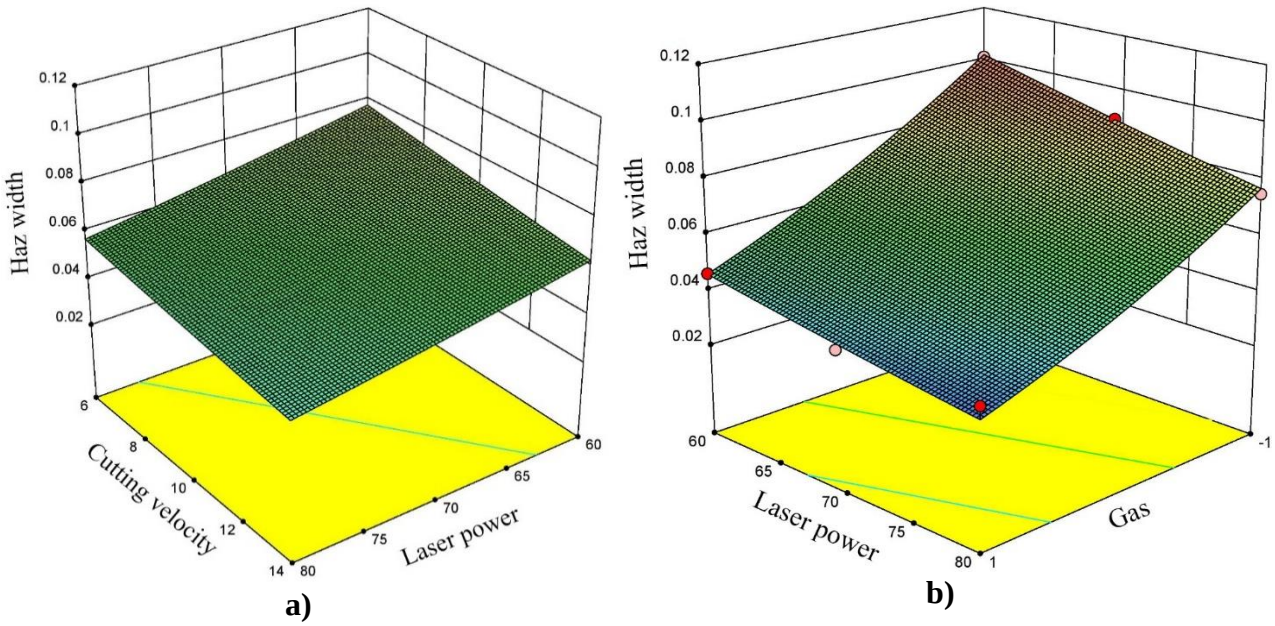

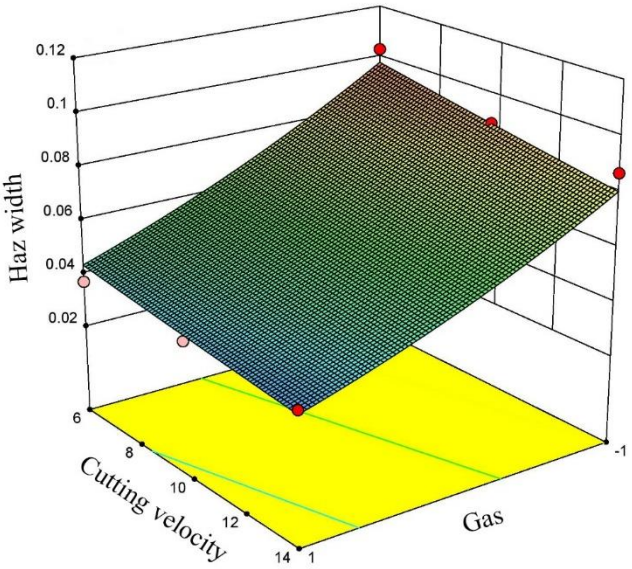

c)

Fig. 4. 3D surface plots of HAZ width in terms of input parameters

3.2. Top kerf width

Table 5 demonstrates ANOVA analysis for top kerf width. The ANOVA table reveals that all main factors are significant and also there is an interaction effect between covering gas and laser power.

Table 5. Analysis of variance (ANOVA) for top kerf width

Source	Sum of Squares	Df	Mean Square	F Value	p-value
Model	0.031	4	7.776E-003	52.03	<0.0001
G	0.017	1	0.017	113.16	<0.0001
P	3.521E-003	1	3.521E-003	23.56	0.0003
V	7.640E-003	1	7.640E-003	51.12	<0.0001
G×P	3.033E-003	1	3.033E-003	20.29	0.0006
Residual	1.943E-003	13	1.495E-004		
Total	0.033	17			
	R-Squared= 94.12%			R-Squared (Adj)= 92.31%	

Equations (5) and (6) are predictive model of top kerf width in terms of coded and actual factors, respectively:

$$(\text{Top kerf width})^{2.7} = +0.098 - 0.031\ G + 0.017\ P - 0.025\ V - 0.016\ G \times P \quad (5)$$

$$(\text{Top kerf width})^{2.7} = +0.040996 + 0.080627\ G + 1.71287E\text{-}00\ 3\ P - 6.30787E\text{-}003\ V - 1.58970E\text{-}003\ G \times P \quad (6)$$

Figure 5 shows perturbation plot of top kerf width. The perturbation plot denotes that increasing laser power leads to increasing top kerf width while holding other input parameters constant. However, increasing cutting velocity results in decreasing top kerf width. Figure 6 displays surface plots of top kerf width in terms of input parameters. Figure 6-a confirms that increasing laser power and decreasing cutting velocity at a time cause wider top kerf which can be explained by heat input concept. From Figure 6-b it can be understood that decreasing cutting velocity without covering gas causes wider top kerf.

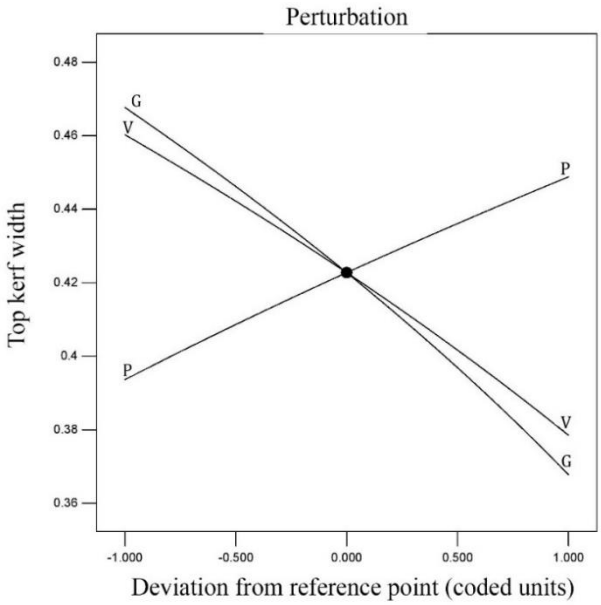

Fig. 5. Perturbation plot of top kerf width

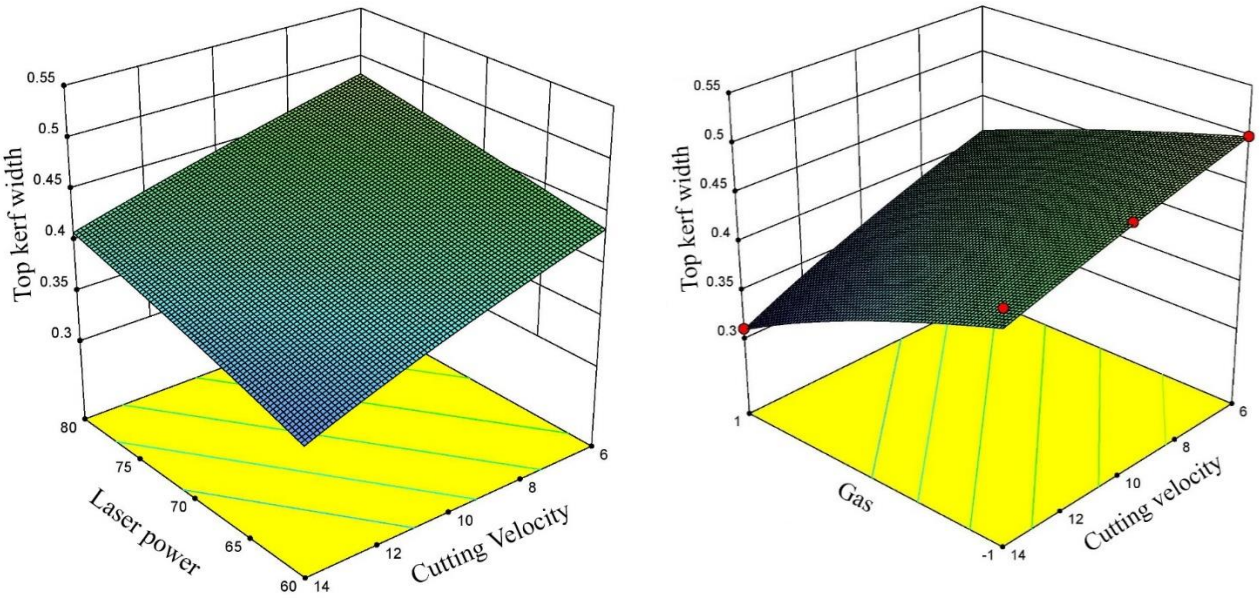

Fig. 6. 3D surface plots of top kerf width in terms of input parameters

3.3. Bottom kerf width

According to analysis of variance on bottom kerf width, Table 6, all the linear parameters are effective and the interaction effects of G × P, and G × V are significants. Equations (7) and (8) are predictive model of HAZ width in terms of coded and actual factors, respectively:

$$(\text{Bottom kerf width})^{-3} = +8.19 + 1.83\ G - 1.89\ P + 3.46\ V + 1.01\ G \times P + 1.56\ G \times V \quad (7)$$

$$(\text{Bottom kerf width})^{-3} = +12.79194 - 9.15917\ G - 0.18916\ P + 0.86429\ V + 0.10118\ G \times P + 0.39076\ G \times V \quad (8)$$

Table 6. Analysis of variance (ANOVA) for bottom kerf width

Source	Sum of Squares	Df	Mean Square	F Value	p-value
Model	288.29	5	57.66	113.09	<0.0001
G	60.33	1	60.33	118.33	<0.0001
P	42.94	1	42.94	84.21	<0.0001
V	143.42	1	143.42	281.30	<0.0001
G×P	12.28	1	12.28	24.09	0.0004
G×V	29.32	1	29.32	57.50	<0.0001
Residual	6.12	12	0.51		
Total	294.41	17			
	R-Squared= 97.92%			R-Squared (Adj)= 97.06%	

The trend of parameters effect on the bottom kerf width, Figure 7, is similar to the top kerf width in Figure 5. Figure 8 displays surface plots of bottom kerf width in terms of input parameters. It can be noted that decreasing cutting velocity without covering gas causes wider bottom kerf.

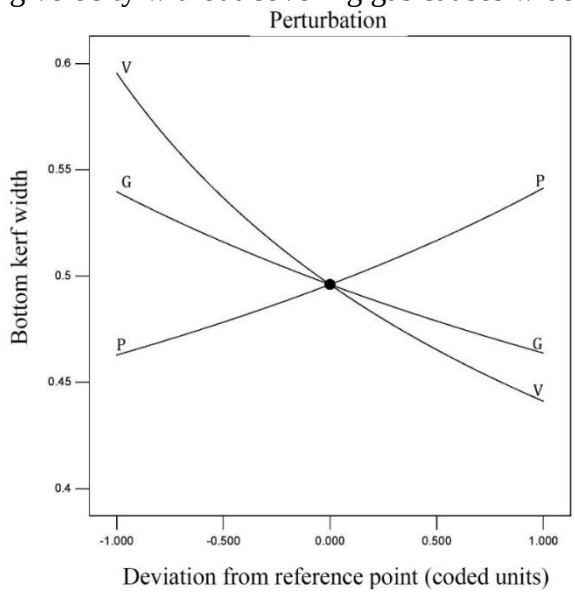

Fig. 7. Perturbation plot of bottom kerf width

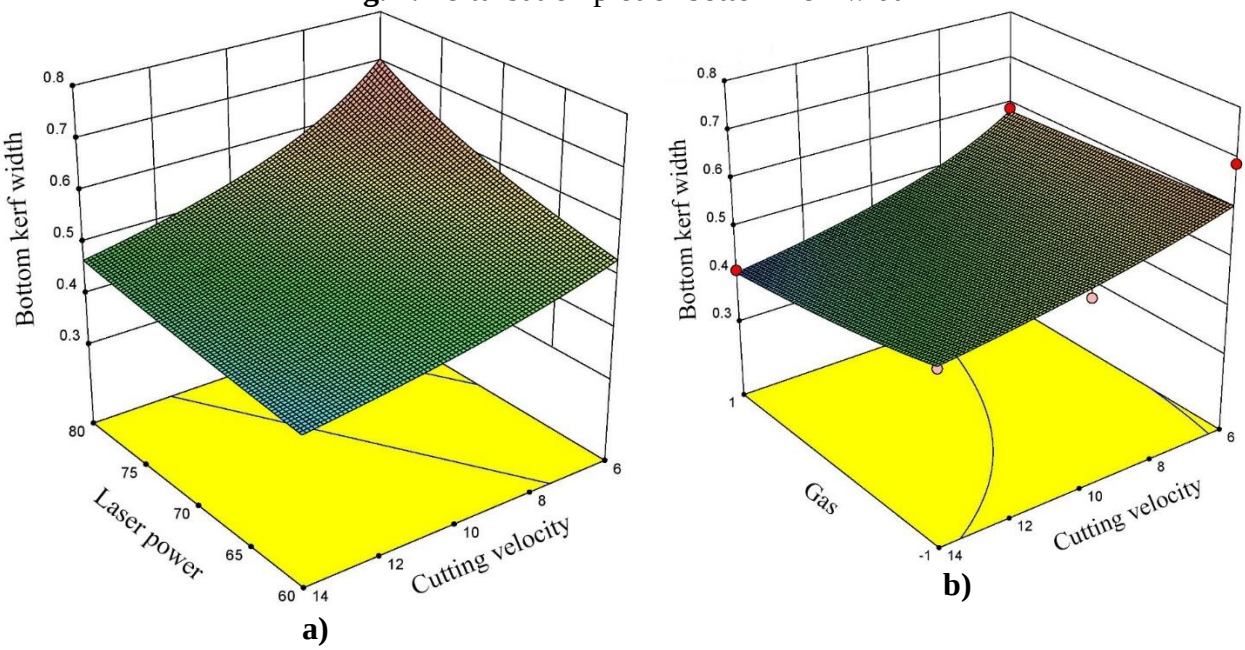

Fig. 8. 3D surface plots of bottom kerf width in terms of input parameters

3.4. Ratio

The ratio is obtained by dividing top kerf width on bottom kerf width. The ideal value for ratio is 1 in this case cutting edges are parallel. The formation of the cutting edges is mainly due to the laser beam divergence in collision with the material which is inevitable. Table 7 demonstrates ANOVA analysis for ratio and indicates that there is no interaction effect between controlled variables.

Table 7. Analysis of variance (ANOVA) for ratio

Source	Sum of Squares	Df	Mean Square	F Value	p-value
Model	3.08	3	1.03	4.71	0.0178
G	0.94	1	0.94	4.32	0.0564
P	0.77	1	0.77	3.53	0.0813
V	1.37	1	1.37	6.29	0.0251
Residual	3.04	14	0.22		
Total	6.12	17			
	R-Squared= 50.25%			R-Squared (Adj)= 39.59%	

Equations (9) and (10) are predictive model of HAZ width in terms of coded and actual factors, respectively:

$$(\text{Ratio})^{-3} = +2.16 + 0.23\ G + 0.25\ P - 0.34\ V \quad (9)$$

$$(\text{Ratio})^{-3} = +1.23799 + 0.22859\ G + 0.025292\ P - 0.084383\ V \quad (10)$$

The cutting velocity coefficient is greater than other coefficients in coded equation, therefore it is more significant than others. Figure 9 shows perturbation plot of ratio. The perturbation plot indicates that increasing cutting velocity leads to increasing ratio and also decreasing laser power results in increasing ratio. Figure 10 displays surface plots of ratio in terms of input parameters. Because the difference between "Pred R-Squared" and "Adj R-Squared" is larger than 0.2 the 3D surface plots are not completely reliable. Nevertheless, evaluation of the 3D surface plots shows that cutting process with covering gas produces lower ratio with higher cutting angle. This phenomenon is probably due to the rapid discharge of the material from the top of the kerf resulted from the covering gas pressure.

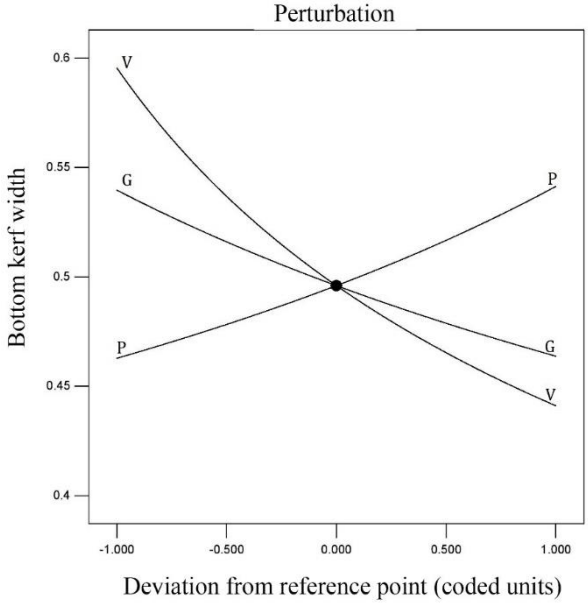

Fig. 9. Perturbation plot of ratio

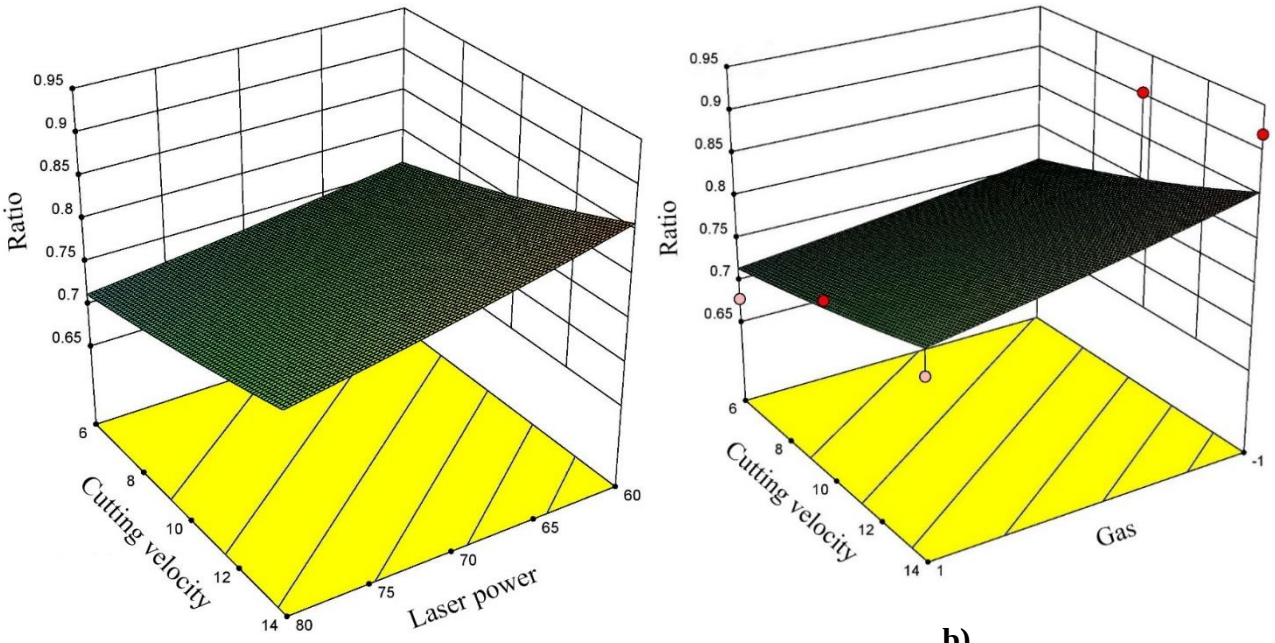

Fig. 10. 3D surface plots of ratio in terms of input parameters

3.5. Dross height

In the melting mechanism, some parts of the melted material adhere to the cutting edges and forms a dross. In the vaporization mechanism due to direct evaporation of the material from the base part, there is no possibility of creating the dross. But in the melting mechanism, some parts of the melted material adhere to the bottom of the cutting walls and causes detrimental effects on the surface quality. Table 8 demonstrates ANOVA analysis for dross height. The ANOVA table also revealed that there are interaction effects between covering gas and laser power and cutting velocity.

Table 8. Analysis of variance (ANOVA) for dross height

Source	Sum of Squares	Df	Mean Square	F Value	p-value
Model	0.14	6	0.023	19.71	<0.0001
G	5.670E-003	1	5.670E-003	4.95	0.0479
P	0.016	1	0.016	13.98	0.0033
V	0.077	1	0.077	67.65	<0.0001
G×P	8.836E-003	1	8.836E-003	7.72	0.0179
G×V	9.472E-003	1	9.472E-003	8.28	0.0150
P×V	0.018	1	0.018	15.65	0.0022
Residual	0.013	11	1.144E-003		
Total	0.15	17			
	R-Squared= 91.49%			R-Squared (Adj)= 86.85%	

Equations (11) and (12) are predictive model of HAZ width in terms of coded and actual factors, respectively:

$$(\text{Dross height})^{0.75} = +0.17 - 0.018\ G - 0.037\ P - 0.080\ V - 0.027\ G \times P + 0.028\ G \times V + 0.047\ P \times V \quad (11)$$

$$(\text{Dross height})^{0.75} = +1.45566 + 0.10196\ G - 0.015481\ P - 0.10289\ V - 2.71359E\text{-}003\ G \times P + 7.02392E\text{-}003\ G \times V + 1.18296E\text{-}003\ P \times V \quad (12)$$

Figure 11 shows perturbation plot of dross height. The perturbation plot demonstrates that increasing each of the variables individually makes the dross height smaller. The significant changes happen by increasing cutting velocity and dross height is much more sensitive to cutting velocity as the deep slop of the V curve shows. Figure 12 displays surface plots of dross height in terms of input parameters. Figure 12-a denotes increasing cutting velocity and decreasing laser power at a time reduce dross height. Figure 12-b suggests that increasing cutting velocity without covering gas reduces dross height. In Figure 12-c shows that by gradual increase of the laser power the cutting mechanism converts from melting to evaporation. It can be mentioned that increasing the laser power while using covering gas causes lower dross height. The compression air helps to easily discharge the melted material from the base part and it also facilitates cutting mechanism from melting to evaporation.

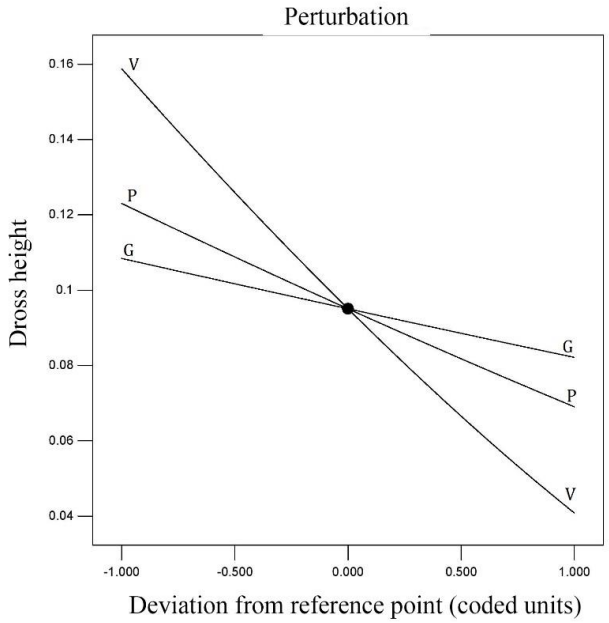

Fig. 11. Perturbation plot of dross height

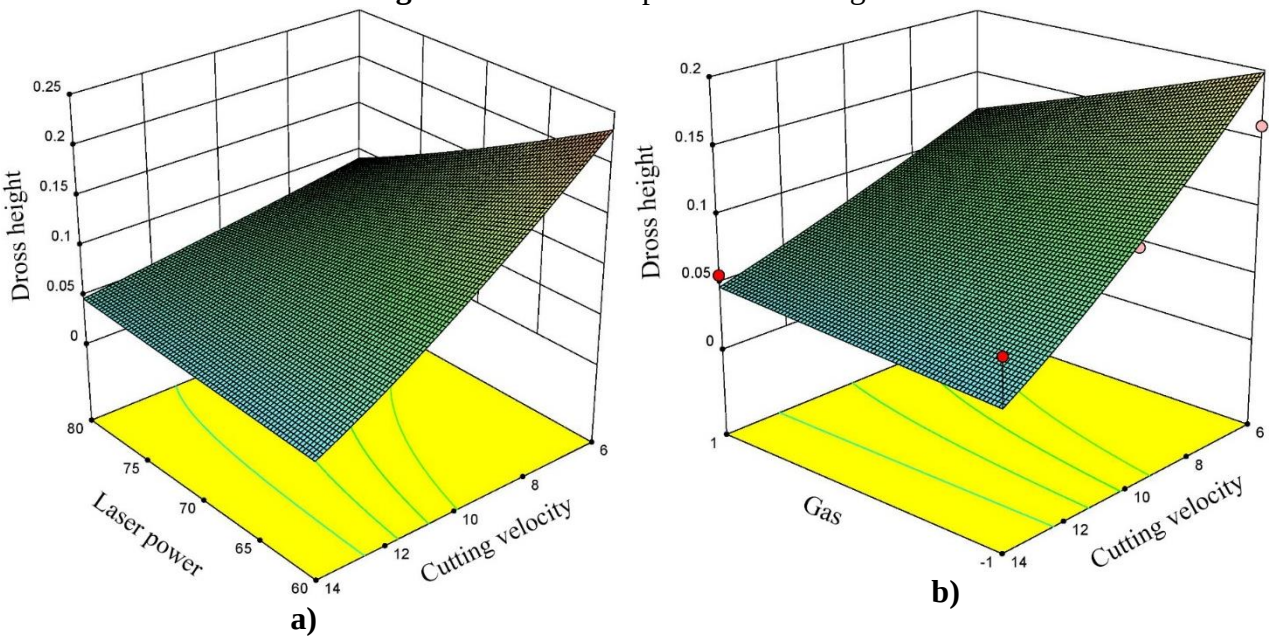

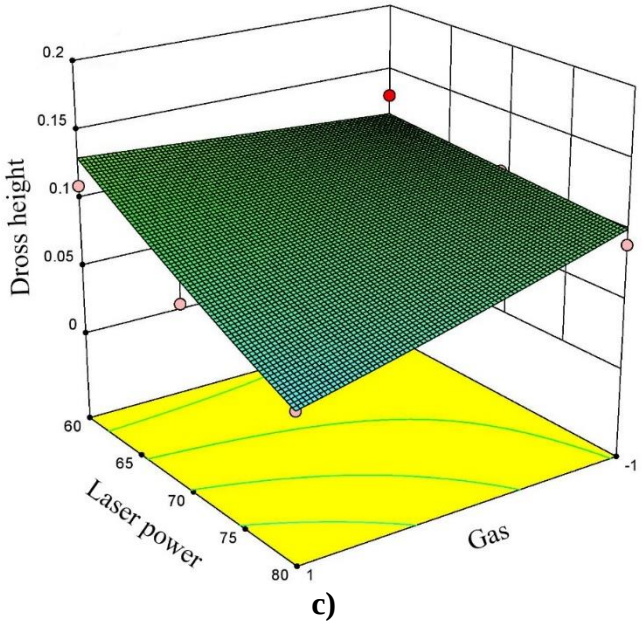

c)

Fig. 12. 3D surface plot of dross height in terms of input parameters

3.6. Numerical Optimization

The objective of the optimization criterion is to attain minimum top kerf width, minimum HAZ, and ideal ratio 1 as the target. Table 9 shows the criterion of numerical optimization. All these criteria results in a better dimensional accuracy of the cutting line. The optimized process parameters to reach the optimization objectives are reported in Table 10. The optimized setting is utilized experimentally for cutting process of the polymer. Results show there is a good agreement between experimental results and RSM predictions. Figure 13 depicts overlay plots which contain the contour plots from each response laid on top of each other. On each contour plot, the desirable area is yellow and undesirable area is grayed-out. In fact, overly plots suggest an adequate process window to attain the high quality cutting process.

Table 9. The criterion of the numerical optimization

Name	Goal	Lower limit	Upper limit	Lower Weight	Upper Weight	Importance
G: Covering gas	is in rang	-1	1	1	1	3
P: Laser power	is in rang	60	80	1	1	3
V: Cutting Velocity	is in rang	6	14	1	1	3
Top kerf width	Minimize	0.31	0.54	1	1	5
Ratio	is target=1	0.6779	1	1	1	5
HAZ width	minimize	0.027	0.108	1	1	5

Table 10. Comparison between Experimental results with RSM

Optimized setting			Desirability	Type of results	Responses		
Covering gas	Laser power	Cutting velocity			Top kerf width	Ratio	HAZ width
1	60	14	0.719	Experimental results	0.333	0.8474	0.038
				RSM results	0.3055	0.8219	0.0405
				Error	8.25 %	3.00%	-6.58%

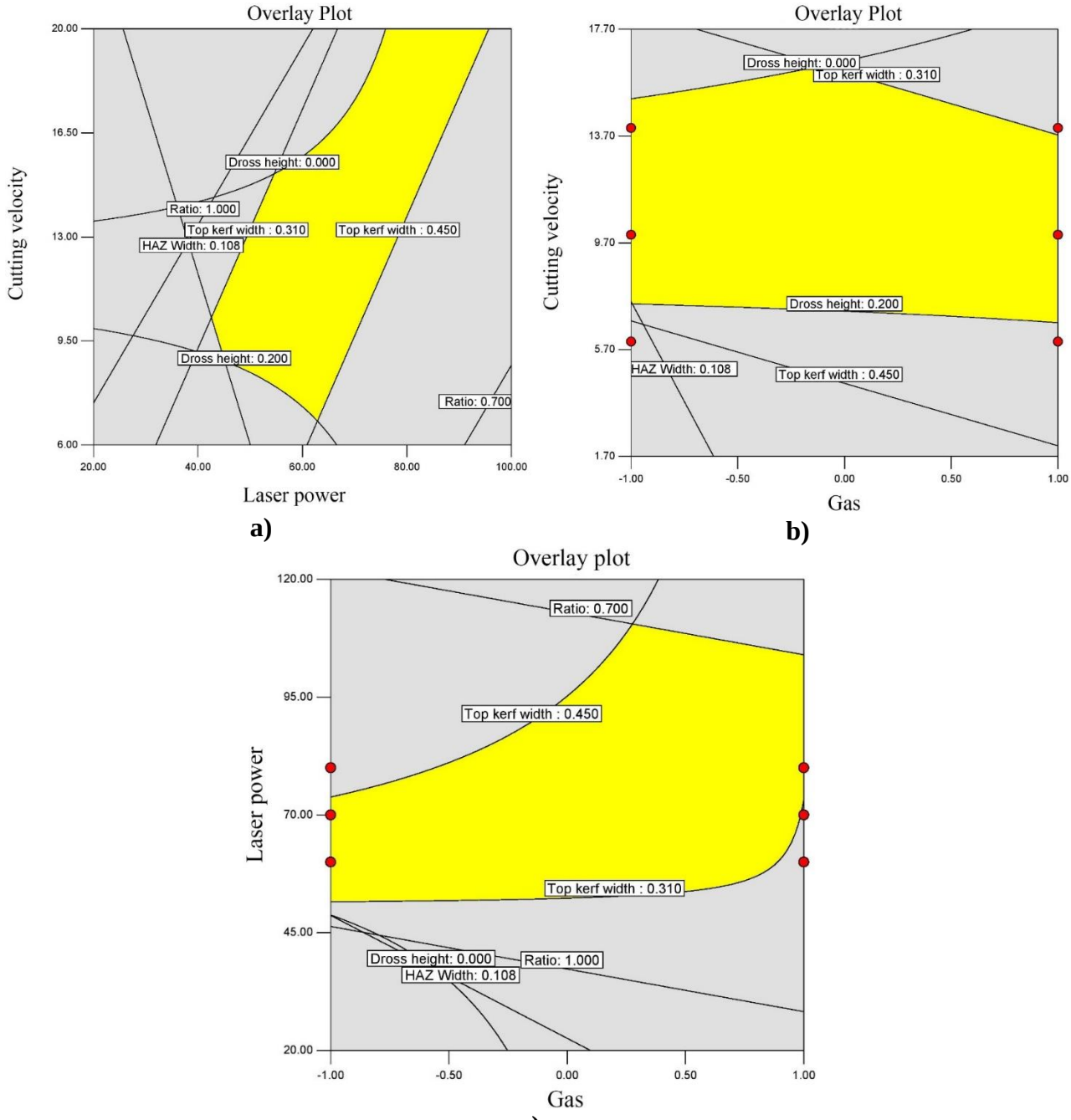

Fig. 13. Overlay contour plots in terms of input parameters

4. Conclusions

In the present research, laser cutting process was accomplished using low power CO_2 laser on extruded polystyrene sheets with thickness of 3 mm based on full factorial Design of experiments. The prominent results can be summarized as follows:

- Increasing the laser power and cutting velocity can help to reduce the heat affected zone, on the other hand using covering gas has a greater effect on controlling and limiting the HAZ width.

- The results showed that in order to increase the ratio, application of higher cutting velocity with lower laser powers is beneficial, but in this case, taking advantages of higher cutting velocity is more effective than the laser power.
- Cutting velocity is the major controlled variable influencing cutting angle and ratio of top kerf width on bottom kerf width.
- Increasing cutting velocity without covering gas reduces dross height. Therefore, unlike HAZ width, using covering gas has an undesirable effect on the dross height.
- The optimized process parameters to improve cutting quality were laser power = 60 (W), cutting velocity = 14 (mm/s) with covering gas achieved by Design- Expert software.

REFERENCES

[1] A. K. Ghavidel, M. Zadshakouyan, Dimensional Accuracy of CNTs/PMMA Parts and Holes Produced by Laser Cutting, *World Academy of Science, Engineering and Technology, International Journal of Mechanical, Aerospace, Industrial, Mechatronic and Manufacturing Engineering,* Vol. 11, No. 10, pp. 1724-1729, 2017.

[2] A. Karimzad Ghavidel, M. Shabgard, H. Biglari, Microscopic and mechanical properties of semi-crystalline and amorphous polymeric parts produced by laser cutting, *Journal of Applied Polymer Science,* Vol. 133, No. 44, pp. 1-11, 2016.

[3] A. Karimzad Ghavidel, A. Navidfar, M. Shabgard, T. Azdast, Role of CO_2 laser cutting conditions on anisotropic properties of nanocomposite contain carbon nanotubes, *Journal of Laser Applications,* Vol. 28, No. 3, pp. 032006-1-9, 2016.

[4]I. Choudhury, S. Shirley, Laser cutting of polymeric materials: an experimental investigation, *Optics & Laser Technology,* Vol. 42, No. 3, pp. 503-508, 2010.

[5]J. P. Davim, N. Barricas, M. Conceicao, C. Oliveira, Some experimental studies on CO_2 laser cutting quality of polymeric materials, *Journal of materials processing technology,* Vol. 198, No. 1, pp. 99-104, 2008.

[6]H. Eltawahni, M. Hagino, K. Benyounis, T. Inoue, A.-G. Olabi, Effect of CO_2 laser cutting process parameters on edge quality and operating cost of AISI316L, *Optics & Laser Technology,* Vol. 44, No. 4, pp. 1068-1082, 2012.

[7] A. K. Ghavidel, T. Azdast, M. R. Shabgard, A. Navidfar, S. M. Shishavan, Effect of carbon nanotubes on laser cutting of multi-walled carbon nanotubes/poly methyl methacrylate nanocomposites, *Optics & Laser Technology,* Vol. 67, pp. 119-124, 2015.

[8] S. Rao, A. Sethi, A. K. Das, N. Mandal, P. Kiran, R. Ghosh, A. Dixit, A. Mandal, Fiber laser cutting of CFRP composites and process optimization through response surface methodology, *Materials and Manufacturing Processes,* pp. 1-10, 2017.

[9] M. Moradi, O. Mehrabi, T. Azdast, K. Y. Benyounis, Enhancement of low power CO_2 laser cutting process for injection molded polycarbonate, *Optics & Laser Technology,* pp. 208-218, 2017.

[10] A.H. Faraji, M. Moradi, M. Goodarzi, P. Colucci, C. Maletta. An investigation on capability of hybrid Nd:YAG laser-TIG welding technology for AA2198 Al-Li alloy. *Optics and Lasers in Engineering*. 96 (September), 1-6. 2017.

[11] A. Hossain, Y. Nukman, M. Hassan, M. Harizam, A. Sifullah, P. Parandoush, A fuzzy logic-based prediction model for kerf width in laser beam machining, *Materials and Manufacturing Processes,* Vol. 31, No. 5, pp. 679-684, 2016.

[12] S. Cicero, T. García, J. A. Álvarez, A. Martín-Meizoso, J. Aldazabal, A. Bannister, A. Klimpel, Definition and validation of Eurocode 3 FAT classes for structural steels containing oxy-fuel, plasma and laser cut holes, *International Journal of Fatigue,* Vol. 87, pp. 50-58, 2016.
[13] A. Hossain, A. Hossain, Y. Nukman, M. Hassan, M. Harizam, A. Sifullah, P. Parandoush, A fuzzy logic-based prediction model for kerf width in laser beam machining, *Materials and Manufacturing Processes,* Vol. 31, No. 5, pp. 679-684, 2016.
[14] E. Haddadi, N. Choupani, F. Abbasi, Investigation on the Effect of Different Pre-Cracking Methods on Fracture Toughness of RT-PMMA, *Latin American Journal of Solids and Structures,* Vol. 13, pp. 2012-2026, 2016.
[15] M. Moradi, O. Mehrabi, T. Azdast, K. Y. Benyounis, Effect of the focal plane position on CO2 laser beam cutting of injection molded polycarbonate sheets, *Proc. SPIE 10150, Second International Seminar on Photonics, Optics, and Its Applications (ISPhOA 2016),* Vol. 10150, pp. 101500F-1-10, 2016.
[16] M. S. Amjadi, E. Foroozmehr, M. Badrossamay, Study of heat-affected zone (HAZ) caused by cutting of Thin Ti-CP Sheet via CW CO_2 Laser, *Modares Mechanical Engineering,* Vol. 17, No. 5, pp. 253-259, 2017.
[17] A. B. Strong, *Plastics: materials and processing,* Prentice Hall, pp. 70-74, 2006.
[18] F. Caiazzo, F. Curcio, G. Daurelio, F. M. C. Minutolo, Laser cutting of different polymeric plastics (PE, PP and PC) by a CO_2 laser beam, *Journal of Materials Processing Technology,* Vol. 159, No. 3, pp. 279-285, 2005.
[19] G. Pastras, A. Fysikopoulos, P. Stavropoulos, G. Chryssolouris, An approach to modelling evaporation pulsed laser drilling and its energy efficiency, *International Journal of Advanced Manufacturing Technology,* Vol. 72, No. 9-12, pp. 1227–1241, 2014.
[20] A. K. Ghavidel, M. Shabgard, T. Azdast, Influence of Alignment and Dispersion Pattern of Carbon Nanotubes in the Polycarbonate and Polystyrene Matrixes on Laser Cutting Workability, *Journal of Laser Micro Nanoengineering,* Vol. 11, No. 2, pp. 266-275, 2016.
[21] M. Mahmoodi, M. Arjmand, U. Sundararaj, S. Park, The electrical conductivity and electromagnetic interference shielding of injection molded multi-walled carbon nanotube/polystyrene composites, *Carbon,* Vol. 50, No. 4, pp. 1455-1464, 2012.
[22] D. W. Van Krevelen, K. Te Nijenhuis, *Properties of polymers: their correlation with chemical structure; their numerical estimation and prediction from additive group contributions,* Elsevier, pp. 73-76, 2009.
[23] H. G. Elias, *Macromolecules: Applications of Polymers*, Volume 4, pp. 111-115, 2009.
[24] M. Mahmoodi, *Electrical, thermal, and machining behaviour of injection moulded polymeric CNT nanocomposites,* Thesis, University of Calgary, pp. 50-54, 2013.